UNSYS digital

Journal of Unmanned System Technology

Controller for Attitude Stabilization with Disturbance Rejection for Steady Hover of Rotary-Wing Flying Robot

Sarbari Datta[†], Umesh Patkar[†], S J Majumder[†], and M C Majumder[‡]

[†]CSIR-CMERI, India

[‡]NIT Durgapur, India

Abstract—This paper presents the course of development, evolving from a standard SISO feedback controller to an augmented controller required for attitude stabilization with disturbance rejection for steady hover of a Rotary Wing Flying Robot. The main objective is to control the dynamic behavior of the robot, which is complex in shape and motion as nonlinear aerodynamic forces and gravity acts on the system. Due to limited accuracy of the dynamic model, the attitude dynamics is conditionally stable where a minimum amount of attitude feedback is required for system stability. To compensate for conditional stability, a controller for both roll and pitch dynamics is developed adopting cascade control loop feedback architecture where INS system feedback is used for outer control loop while the gyro feedback is adopted for the inner control loop to attain a high bandwidth, ensuring attitude stability with accelerated response required for steady hover. The provided solution is tested on HIROBO Scheadu50 model and the system performance is analyzed during hover using the proposed controller. Through taut integration of simulation and flight-test validation, a controller is developed that is sufficiently accurate, quite effective and simple enough for handling complex and changing rotorcraft dynamics in hover.

Keywords—Attitude stabilization, gyro feedback, dynamic model.

I. Introduction

A new variety of mobile robots often called as flying robots have shown a lot a promise in overcoming the limitations of conventional mobile robots. Flying operation has opened up new opportunities to robotically perform field services and tasks like search and rescue, observation and mapping. Rotary wing flying robots (RWFR) deserve special interest for their low-altitude flight capabilities suitable for all weather conditions featuring vertical take-off/landing from any point, hover and way point navigation. For this high degree of maneuverability, these types of mobile robots have more potential than fixed-wing air vehicles. The objective of CSIR-CMERI's RWFR research is on hovering for close inspection of bridges and open cast mines and on terrain aided navigation for exploration and geological surveys i.e. to map out tracts of distant terrain to explore for potential mineral deposits. Here, the focus is on generating a trajectory to ensure optimal coverage in minimal time to be traversed at low altitude over long distances by carrying a suitable payload of scientific equipment capable of storing and transmitting information with other aerial and land based robotic system working in the same network to generate composite information to be used by the central command station.

Corresponding author: Sarbari Datta (e-mail: sdatta@cmeri.res.in).
This paper was submitted on November 16, 2013; revised on September 29, 2013; and accepted on December 30, 2014.

As stated earlier, due to limited accuracy of the dynamic model, which is complex in shape and motion as nonlinear aerodynamic forces and gravity acts on the system, a minimum amount of attitude feedback is required for system stability. To compensate for conditional stability, a controller for both roll and pitch dynamics is developed at CSIR-CMERI adopting cascade control loop feedback architecture where INS system feedback is used for outer control loop while the gyro feedback is adopted for the inner control loop for an attitude reference input, to attain a high bandwidth, ensuring attitude stability with accelerated response required for a steady hover.

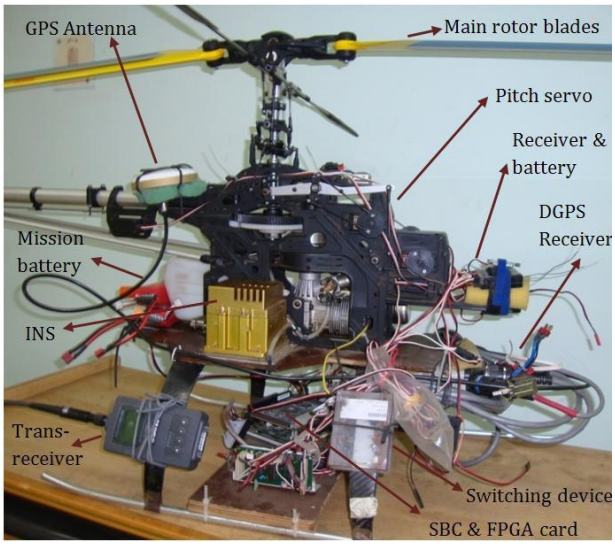

Figure 1 CMERI RWFR equipped with SBC interfacing INS and GPS for hovering

Several methods have been reported for attitude control, a key factor for steady hover. Wu, et al. describe an attitude control method for unmanned rotary wing vehicle based on adaptive output feedback where the control system satisfies

output feedback linearization conditions and the model is considered as the diffeomorphism of the nonlinear system. A linear controller and adaptive neural networks are then designed to cancel the model errors produced by nonlinearity, uncertainty and disturbance [1]. Sakamoto, et al. have used robust PID controllers, designed iteratively to give satisfactory performance in step tracking and stability [2]. Zhou, et al. report a linear time-invariant model extracted by frequency identification technique and developed a controller using multi-loop control method for steady hover, an approach similar to our proposed controller [3]. Their attitude control system consists of a linear PD controller and a feed-forward neural network compensator. Our focus is on Kalman filter -based attitude controller featuring optimal approximation for compensating against the error caused by the deficiency of full knowledge of rotary wing robot dynamics. The controller performance is analyzed during hover operation from field trials carried out on Hirobo Scheadu50 model shown in **Figure 1**.

II. RWFR Architecture with Physical Description

Suitable system architecture is devised for implementing the stated controller for attitude stabilization. For flight computer system, RWFR is equipped with Pentium-M 1.6 GHz -based SBC with 1 MB cache and PC/104+ expansion site running on Windows operating system. A PC/104+ -based high-speed digital FPGA card is mounted on the SBC to allow for high-speed data throughput. This includes generating PWM outputs using programmable clocks for controlling the digital servos. For gyro feedback, RWFR in **Figure 2** has angular velocity gyros mounted on lateral and longitudinal axes; for sensor feedback, Crossbow's inertial navigational sensor NAV440 is interfaced to the RWFR system. NAV440 is mounted underneath the chassis as close to the system center of gravity (CG) as possible. This minimizes any lever effect that can contribute to direct errors in measured rotation relative to the system axis. For absolute measurements, Novatel's FlexPak GPS receiver with antenna is used for absolute positioning and KVH C-100 flux gate compass is used for absolute heading. System architecture with layout details in **Figure 3** and **Figure 4** shows the dual mode control of RWFR. The manual control is through a remote controlled radio system consisting of a transmitter and a 10-channel receiver. Of the 10 channels, 8-channels are used. Four channels are used for controlling aileron, elevator, rudder, and throttle/pitch, and three are used as aileron, elevator and rudder gyro sensitivity channels. The final channel acts as a system mode selector that switches between the control signals from transmitter and RWFR computer system and route them to respective servos. This gives the user the ability to activate and deactivate the auto controller and manually control the RWFR as and when necessary. In the auto or computer-controlled mode, a base station or field computer monitors the RWFR. The field computer communicates with RWFR through 100 Mbps WLAN link using TCP/IP protocol. The field computer acts as a client by latching on the RWFR server. It monitors all mission data from navigational sensors mounted on RWFR as stated above and displays the series of images grabbed by the onboard camera. In case of any aberration in the sensor data as monitored on the field computer, the mission is aborted by deactivating the auto controller.

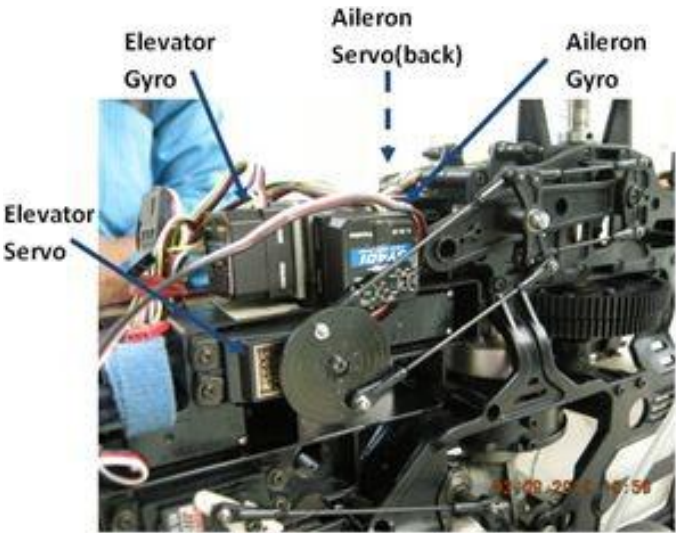

Figure 2 Angular velocity gyros mounted on lateral and longitudinal axes

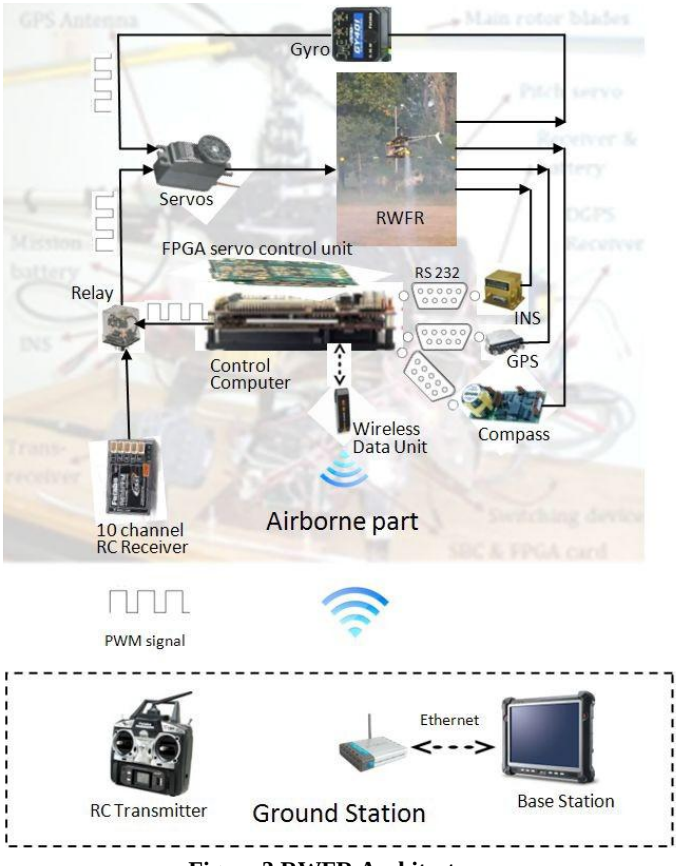

Figure 3 RWFR Architecture

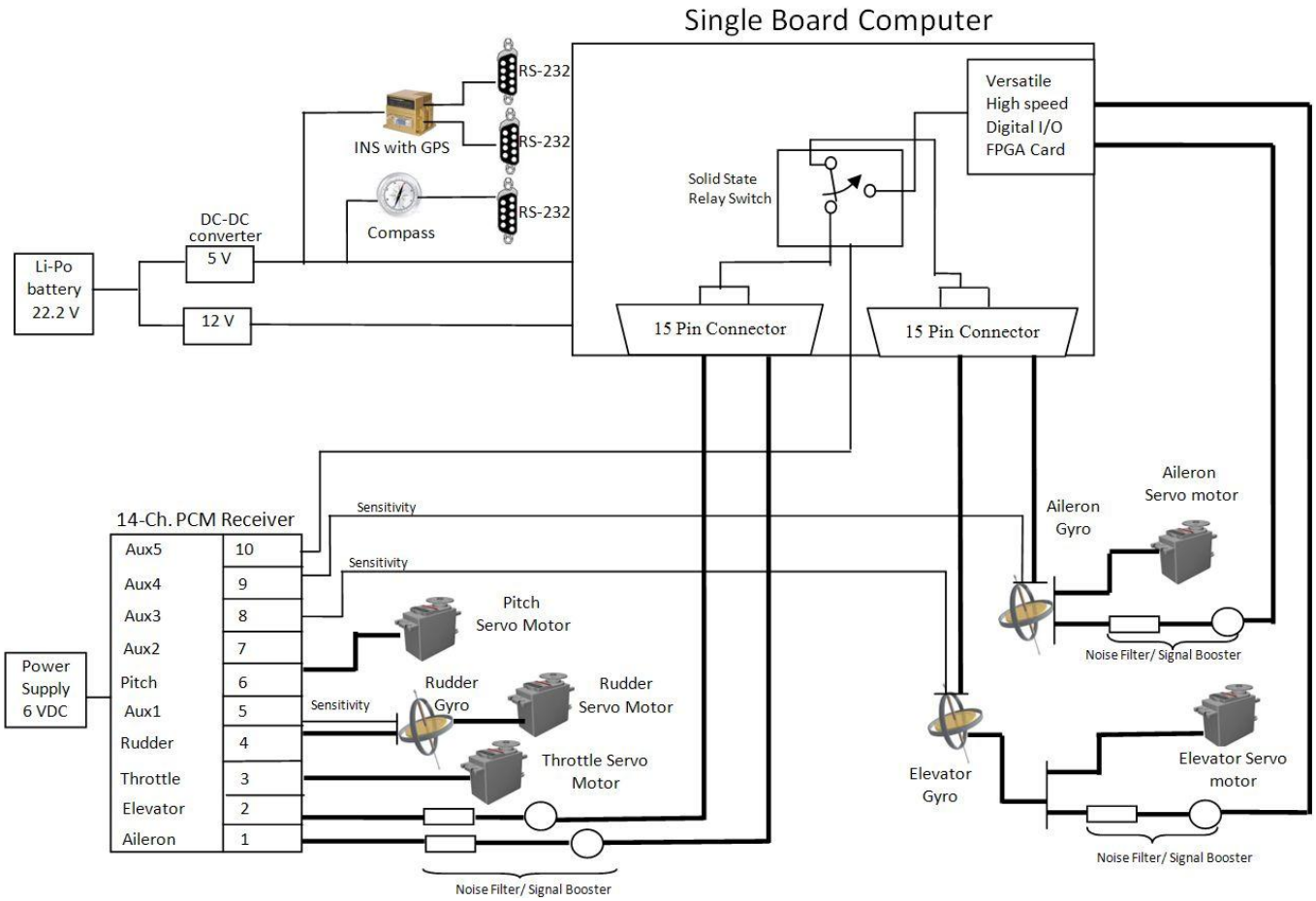

Figure 4 Schematic layout of RWFR

III. RWFR Attitude Controller

To address the model stability, system identification modeling is used for autonomous hover. It allows characterization of rotorcraft dynamics from experimental data by integration of different design steps through modeling of linear state-space developed from combination of:

- First principle knowledge, physical insight and frequency response analysis
- Performance analysis through small perturbations
- Control design with open and closed-loop validation
- Flight test validation

It provides blending of mechanical systems (airframe, rotor mechanization), electrical components (actuators and sensors) and digital components (flight computers, micro-controllers). The model is valid in the vicinity of an operating point like hover to slow speed flight, forward flight and fast-forward flight.

A. Modeling of Attitude Controller using System Identification

Attitude controller is composed of attitude angles and angular rate feedbacks. These control loops track the reference roll and pitch attitude angles for position holds. Data is collected using lateral and longitudinal feedback in response to lateral and longitudinal cyclic control inputs to digital servos. The position and attitude of RWFR are controlled through four primary control input. The model is linearized about the hover operating point which acts as the control envelope for flight operating condition. Linear SISO controller structure is used within this envelope, one for each of the desired outputs to be controlled [4],[5], neglecting inter-axis coupling. This condition is valid for small perturbations from equilibrium point in a quasi-stable state but if the vehicle moves away from its equilibrium point, dynamic performance can degrade severely if inter-axis coupling is neglected.

For experimental trial, RWFR system was first mounted on a test rig, shown in **Figure 5**. The system parameters were tuned for field trial by adding noise filters and signal boosters, changing 50cc engine to 55cc engine, increasing the nitro content of the fuel to 30 % and replacing existing swash-plate structure with a metallic structure for better system performance. After tuning the controller on the test rig, field trial was carried out on the system to test the controller -aided attitude stabilization. **Figure 6** shows an unaided flight using a standard attitude controller used for performance mapping for attitude stabilization.

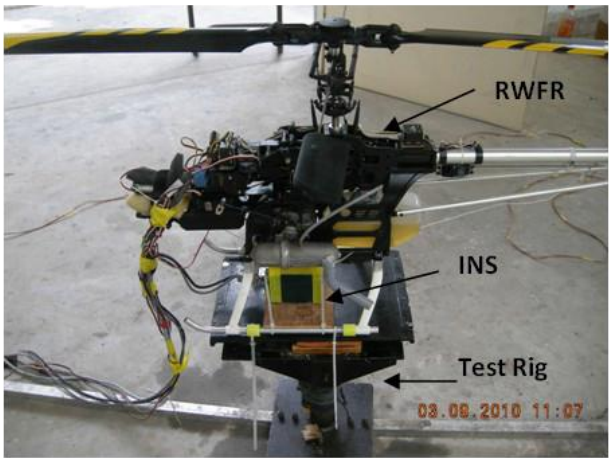

Figure 5 RWFR on test-rig

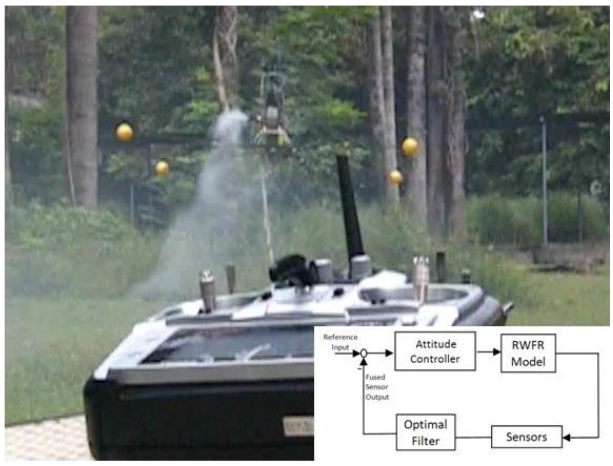

Figure 6 Unaided flight using standard attitude controller shown in the inset

During offline processing of collected data, a linear time invariant auto-regressive model is employed for system identification to record the dynamic behavior of the attitude controller. When analyzing the root locus plot, bode plot, and Nyquist plot, it is seen that the system is unstable violating stability margin criteria [6]. A high attitude control bandwidth is necessary for fast vehicle attitude response to an attitude reference input where the inner control loop has a higher bandwidth than the outer control loop. To achieve this, we propose fast-acting gyros for inner control loop and sensor-based attitude angle control in the outer control loop. This approach gives another added tier of robust feedback control of RWFR with a higher bandwidth.

B. RWFR Attitude Controller for Attitude Stabilization with Disturbance Rejection for Steady Hover

An attitude controller with cascade control loop architecture is devised for attitude stabilization with improved disturbance rejection as the cascade loop is faster than simply the INS feedback, and it reduces the problem of correcting the output only by feedback, i.e., the inner control loop has a higher bandwidth than the outer control loop. The gyros in the inner control loop sense the disturbance that affect the output before they actually do affect the output, thus introduce corrective control to mitigate these disturbances on the output. This novel approach gives another added tier of feedback control of RWFR with a higher bandwidth. **Figure 7** shows the block diagram cascade control loop architecture of RWFR attitude controller where the gyro data is fused with INS data, shown in RWFR architecture of **Figure 3**.

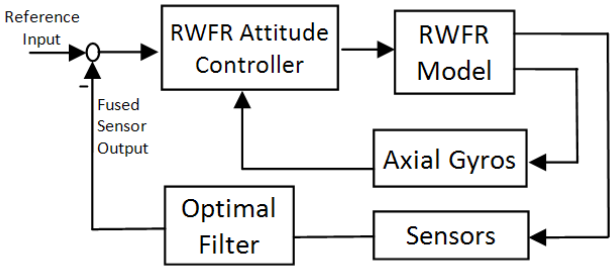

Figure 7 Block diagram of RWFR attitude controller

Figure 4 illustrates the RWFR attitude control scheme for continuous compensation from linear SISO controllers to control the nonlinear dynamics of RWFR during the unaided flight. ϕ_s, θ_s, p_s, and q_s are system roll, pitch, roll rate and pitch rate respectively and p_f and q_f are inner loop gyro feedback roll rate and pitch rate respectively with full state space representation

$$\boldsymbol{x}_s(t) = \begin{bmatrix} \phi_s(t) \\ \theta_s(t) \\ p_s(t) \\ q_s(t) \\ p_f(t) \\ q_f(t) \end{bmatrix} \tag{1}$$

ϕ_f and θ_f are integrated roll and pitch gyro feedback of inner gyro loop feedback. Due to tight control loops required for steady hover, the system roll rate p_s and pitch rate q_s from gyro output of the INS, which provide very good high frequency information, are used. But because of inherent gyro characteristics, the system drifts at a slow rate and errors creep in, which grow with time. To correct the drift i.e. for bounding or damping these errors, we propose fast-acting gyros for inner control loop and sensor-based attitude angle control in the outer control loop. The gyros sense the disturbance that affect the output before they actually do affect the output, thus introduce corrective control to mitigate these disturbances on the output. This novel approach gives another added tier of feedback control of RWFR with a higher bandwidth.

The objective is to optimally estimate attitude information $\hat{\phi}_f(t)$ and $\hat{\theta}_f(t)$ obtained by fusing the system model with the feedback model as shown in **Figure 8**. To start with, is to measure the difference

$$\begin{aligned} \delta\phi_f(t) &= \phi_f(t) + \phi_s(t) \\ \delta\theta_f(t) &= \theta_f(t) + \theta_s(t) \end{aligned} \tag{2}$$

for all time t of interest for lateral state vector $\boldsymbol{x}_{\phi_f}(t) = \begin{bmatrix}\phi_s(t)\\ p_f(t)\end{bmatrix}$ for estimating roll angle $\hat{\phi}_f(t)$, and longitudinal state vector $\boldsymbol{x}_{\theta_f}(t) = \begin{bmatrix}\theta_s(t)\\ q_f(t)\end{bmatrix}$ for estimating pitch angle $\hat{\theta}_f(t)$. Optimally estimated attitude information for RWFR is

$$\begin{aligned}\hat{\phi}_f(t) &= \phi_f(t) - \delta\hat{\phi}_s(t)\\ \hat{\theta}_f(t) &= \theta_f(t) - \delta\hat{\theta}_s(t)\end{aligned} \tag{3}$$

where $\delta\hat{\phi}_s(t)$ and $\delta\hat{\theta}_s(t)$ are estimates of $\delta\phi_s(t)$ and $\delta\theta_s(t)$ given as

$$\begin{aligned}\delta\phi_s(t) &= \phi_i(t) - \phi_s(t)\\ \delta\theta_s(t) &= \theta_i(t) - \theta_s(t)\end{aligned} \tag{4}$$

for all time t of interest for lateral state vector $\boldsymbol{x}_{\phi_s}(t) = \begin{bmatrix}\phi_s(t)\\ p_s(t)\end{bmatrix}$ and longitudinal state vector $\boldsymbol{x}_{\theta_s}(t) = \begin{bmatrix}\theta_s(t)\\ q_s(t)\end{bmatrix}$.

Given the perturbative input control vector $\boldsymbol{u}_f = [\delta_{\text{lat}_f} \quad \delta_{\text{lon}_f}]^{\text{T}}$, the state space model of the RWFR attitude controller is

$$\begin{bmatrix}\dot{\phi}_s(t)\\ \dot{p}_f(t)\end{bmatrix} = \boldsymbol{A}_{\text{lat}}\begin{bmatrix}\phi_s(t)\\ p_f(t)\end{bmatrix} + \boldsymbol{B}_{\text{lat}}\delta_{\text{lat}_f}$$
$$\boldsymbol{y}_{\text{lat}} = \boldsymbol{C}_{\text{lat}}\begin{bmatrix}\phi_s(t)\\ p_f(t)\end{bmatrix} \tag{5}$$

$$\begin{bmatrix}\dot{\theta}_s(t)\\ \dot{q}_f(t)\end{bmatrix} = \boldsymbol{A}_{\text{lon}}\begin{bmatrix}\theta_s(t)\\ q_f(t)\end{bmatrix} + \boldsymbol{B}_{\text{lon}}\delta_{\text{lon}_f}$$
$$\boldsymbol{y}_{\text{lon}} = \boldsymbol{C}_{\text{lon}}\begin{bmatrix}\theta_s(t)\\ q_f(t)\end{bmatrix} \tag{6}$$

where $\boldsymbol{A}$, $\boldsymbol{B}$, and $\boldsymbol{C}$ are system, input, and output matrices represented as $\begin{bmatrix}0 & 1\\ 0 & 1\end{bmatrix}$, $\begin{bmatrix}0\\ 1\end{bmatrix}$, and $[1 \quad 0]$, respectively.

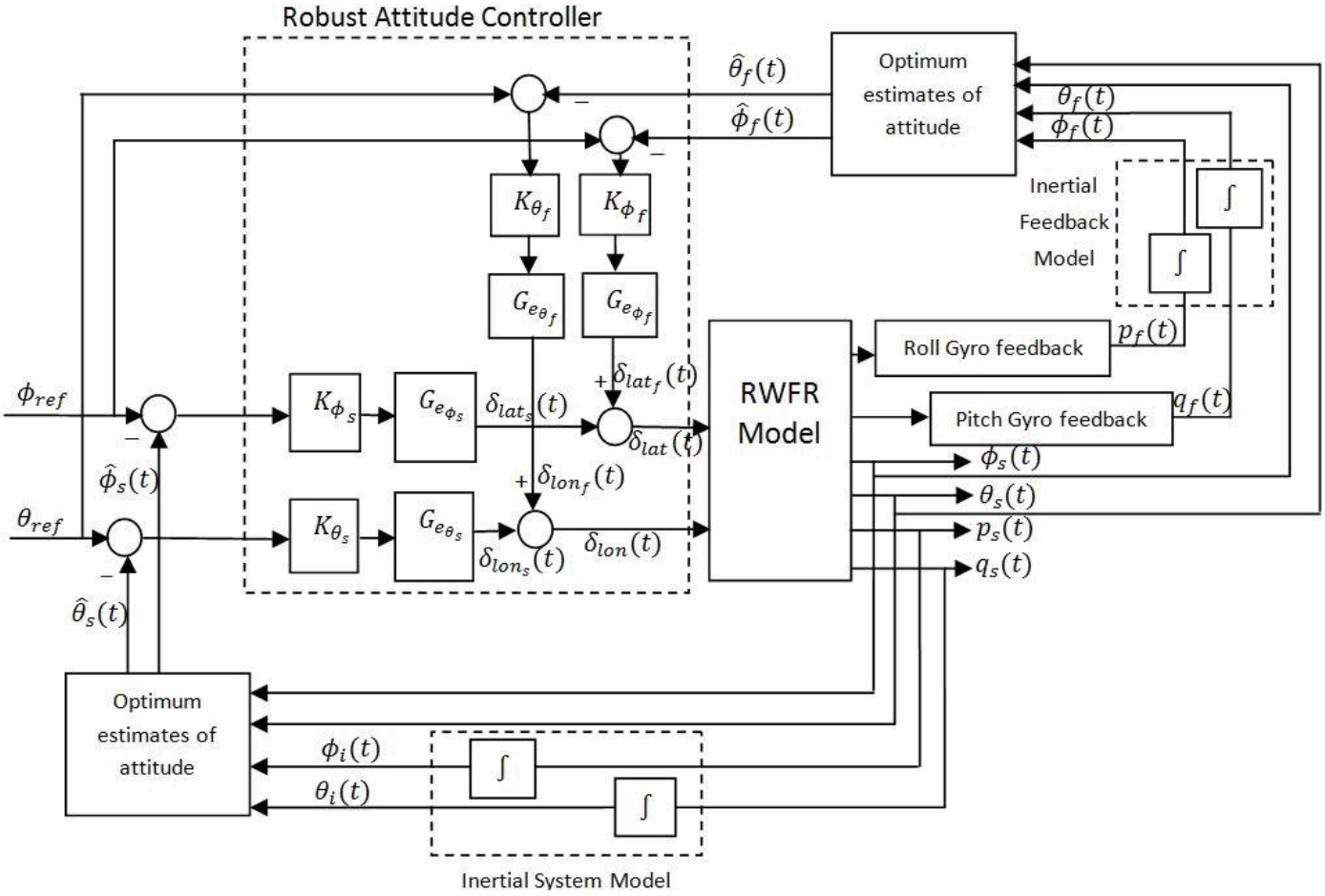

Figure 8 RWFR Attitude control scheme

The first step in designing a controller for each degree of freedom is to determine the transfer function $G_{e_{\phi_f}}(s)$ describing the open-loop roll angle response ϕ_s to the lateral input δ_{lat_f}, and $G_{e_{\theta_f}}(s)$ describing the open-loop pitch angle response θ_s to the longitudinal input δ_{lon_f} which is given as

$$\begin{aligned} G_{e_{\phi_f}}(s) &= \boldsymbol{C}_{\text{lat}}[s\boldsymbol{I} - \boldsymbol{A}_{\text{lat}}]^{-1}\boldsymbol{B}_{\text{lat}} \\ G_{e_{\theta_f}}(s) &= \boldsymbol{C}_{\text{lon}}[s\boldsymbol{I} - \boldsymbol{A}_{\text{lon}}]^{-1}\boldsymbol{B}_{\text{lon}} \end{aligned} \tag{7}$$

where $\boldsymbol{I}$ is the unity matrix. Then, the open loop feedback transfer function for roll and pitch angle response to the reference roll and pitch commands are given by [6]

$$\begin{aligned} T_{\phi_f,\phi_{\text{ref,ol}}} &= K_{\phi_f}(s)G_{e_{\phi_f}}(s) \\ T_{\theta_f,\theta_{\text{ref,ol}}} &= K_{\theta_f}(s)G_{e_{\theta_f}}(s) \end{aligned} \tag{8}$$

where $K_{\phi_f}(s)$ and $K_{\theta_f}(s)$ act as the dynamic compensators necessary to reshape the filter by adding to the open-loop transfer function $G_{e_{\phi_f}}(s)$ and $G_{e_{\theta_f}}(s)$. $K_{\phi_f}(s)$ and $K_{\theta_f}(s)$ act as dynamic compensators and are chosen as high-pass filters to improve the transient response, to raise bandwidth and to increase the speed of response, all essential criteria for stability of the plant cited above.

Finally, the closed loop system feedback transfer function for enhancing the performance of RWFR becomes [6]

$$\begin{aligned} T_{\phi_f,\phi_{\text{ref,ol}}} &= 1 + K_{\phi_s}(s)\frac{G_{e_{\phi_f}}(s)K_{\phi_f}(s)}{1 + G_{e_{\phi_f}}(s)K_{\phi_f}(s)}G_{e_{\phi_s}}(s) \\ T_{\theta_f,\theta_{\text{ref,ol}}} &= 1 + K_{\theta_s}(s)\frac{G_{e_{\theta_f}}(s)K_{\theta_f}(s)}{1 + G_{e_{\theta_f}}(s)K_{\theta_f}(s)}G_{e_{\theta_s}}(s) \end{aligned} \tag{9}$$

IV. Results and Discussion

Hover condition modeling assumes RWFR dynamics can be approximated by rigid-body dynamics and that the coupling between the forces and moments can be neglected. Through taut integration of simulation, control and flight-test validation, system performance of RWFR with augmented attitude control during hover is evaluated. **Figure 9** shows the field trial of Hirobo Scheadu50 model where a binary image of landing pads (shown in the inset) is tracked for measuring lateral and longitudinal deviations as depicted in **Figure 10**, and the system response of RWFR to the augmented attitude controller is examined.

Figure 11(a) shows the bode plot of lateral axis control using the new scheme using processed offline test data collected from field trials. **Figure 11(b)** shows an over-damped system with a steady state error. One way to eliminate steady state error is to add an integrator to the response such that

$$K_{\phi_s}(z) = K_{\phi_s}(z)\frac{1}{1 - z^{-1}} \tag{10}$$

After adding the integrator, the system response is still sluggish as shown in **Figure 11(c)**. The simplest approach for speeding up the system response time is to adjust the bandwidth by increasing the gain of the compensator as shown in **Figure 11(d)** given as

$$K_{\phi_s}(z) = K_{\phi_s}(z)C(z)\frac{1}{1 - z^{-1}} \tag{11}$$

where $C(z)$ (gain of the compensator) > 1 but it does not yield a very good system response. To limit the rise time within 0.5 seconds, and lessen the settling time without compensating stability of the system, only option is to add dynamics to the compensator and one possible solution is to add lead network to bandwidth the compensator. The basic phase lead compensator is a high pass filter and it is utilized to improve the transient response, to raise bandwidth and to increase the speed of response, all essential criteria for the system response of the plant cited above. It consists of a gain, one pole and one zero. The major characteristic of the lead compensator is the positive phase shift in the intermediate frequencies. Proper design of the compensator requires placing the compensator pole and zero appropriately so that the benefits of the positive phase shift are obtained and magnitude shift is accounted for. For the given system after adding dynamic compensator, the robust attitude controller becomes

$$K_{\phi_s}(z) = K_{\phi_s}(z)C(z)D(z)\frac{1}{1 - z^{-1}} \tag{12}$$

where $D(z) = k\frac{1+a_0z^{-1}}{1+b_0z^{-1}}$ and $a_0 < 1$ and $b_0 < 1$.

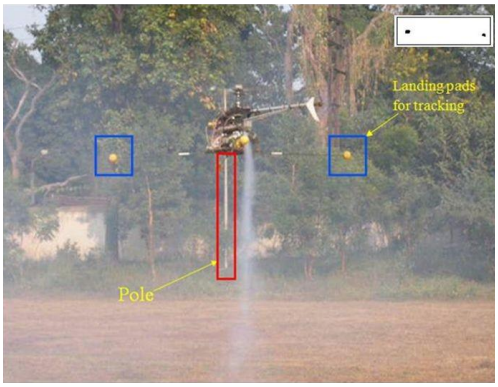

Figure 9 RWFR hovering with the pole in the backdrop acting as the reference; binary image of the landing pad for tracking (inset)

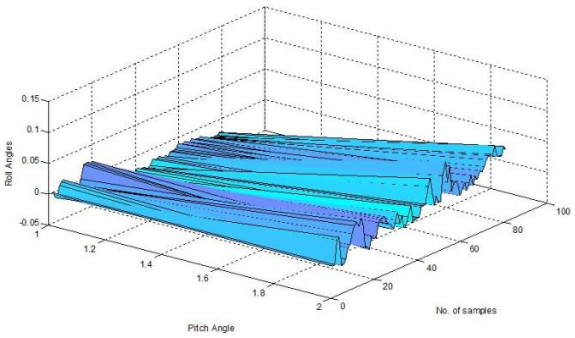

Figure 10 Roll and pitch deviations while hovering

Figure 11(e) and **Figure 11(f)** show the final result in roll and pitch direction respectively after tuning the lead network which meets the criteria for system rise time and settling time without compensating for system stability.

Hover condition modeling assumes RWFR dynamics can be approximated by rigid-body dynamics, and that the coupling between the forces and moments can be neglected. Through taut integration with simulation, control and flight test validation on Hirobo Scheadu50 model, a controller is developed that is sufficiently accurate, quite effective and simple enough for handling complex and changing rotorcraft dynamics in hover.

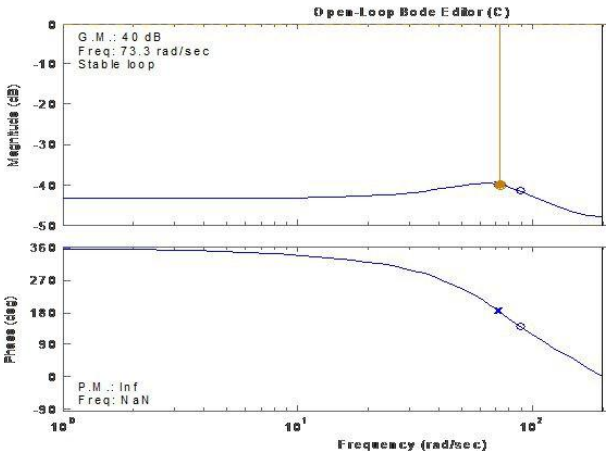

(a) Open loop bode plot

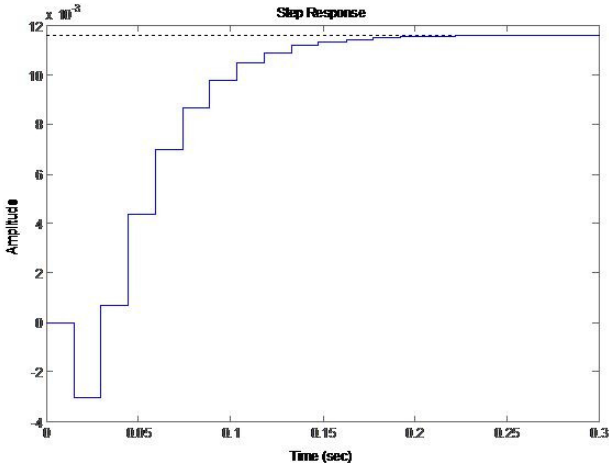

(b) Initial transient response

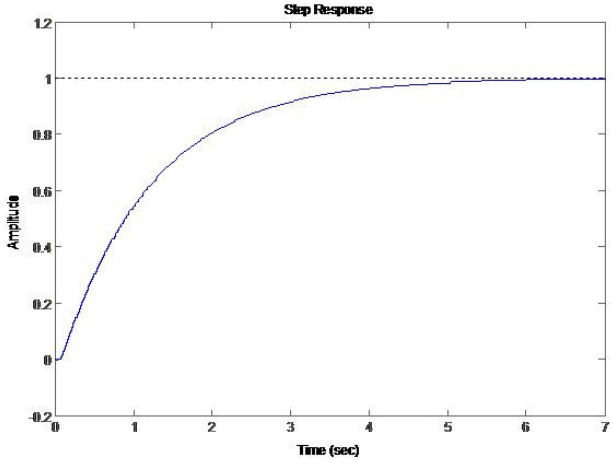

(c) Transient response after adding integrator

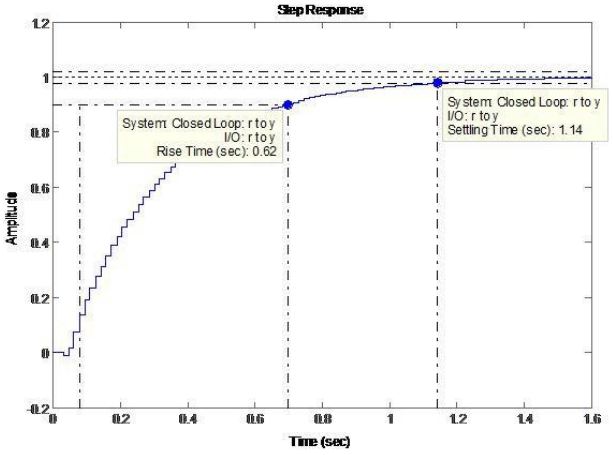

(d) Transient response with increased bandwidth

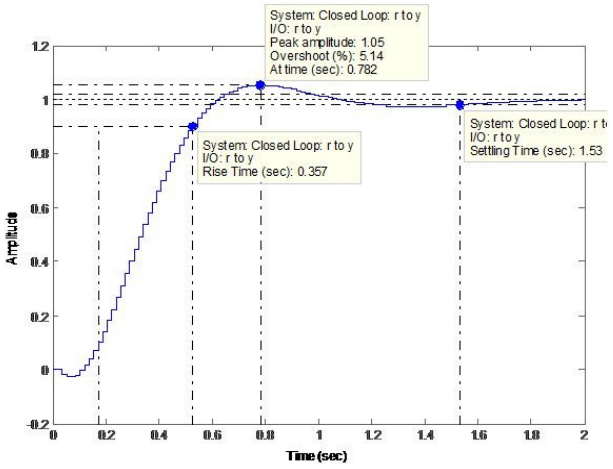

(e) Transient response with lead compensator for lat. control

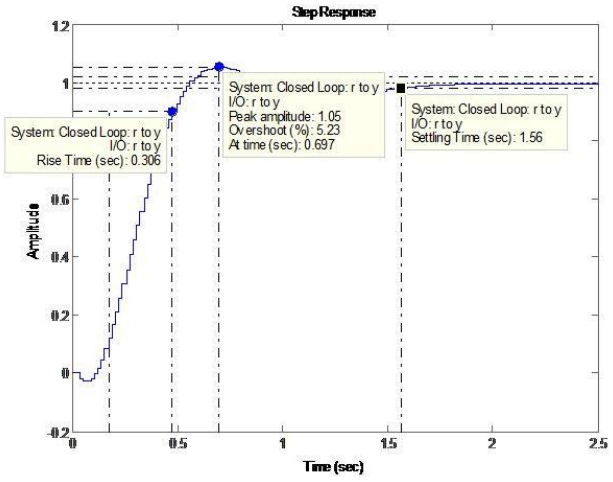

(f) Transient response with lead compensator for long. control

Figure 11

Figure 12 represents the system response of RWFR regarding angular change and angular rate of change. The observation from the gradient based representation of robust attitude controller is that the system is more responsive to perturbations, thus more attuned to correct itself faster than the standard attitude controller where the system response is more flat and thus immune to change. Finally, **Figure 13** compares the performance of the attitude controller with and without gyro feedback.

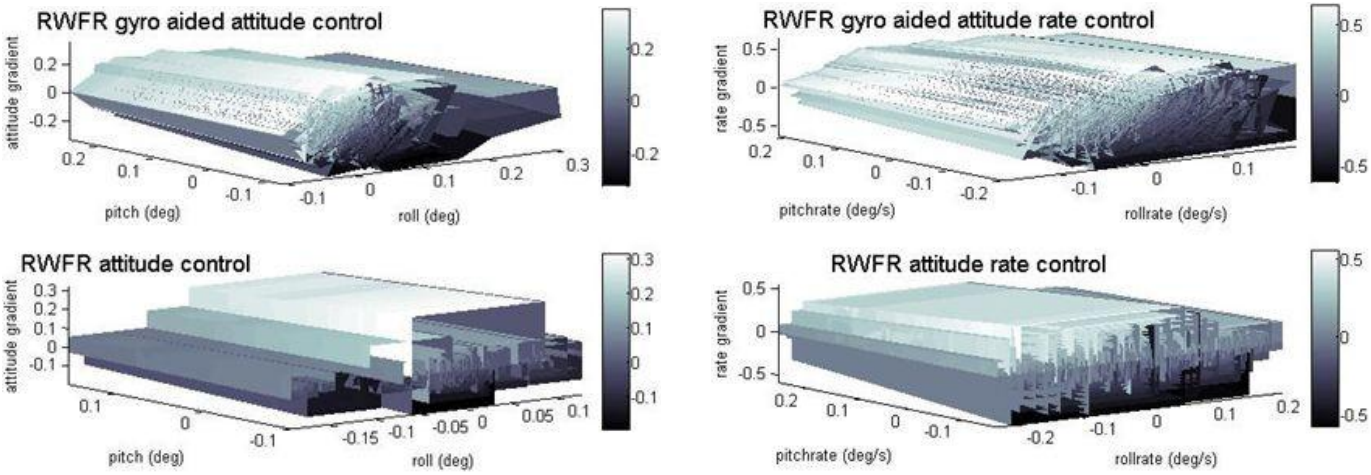

Figure 12 System response of RWFR attitude controller in hover

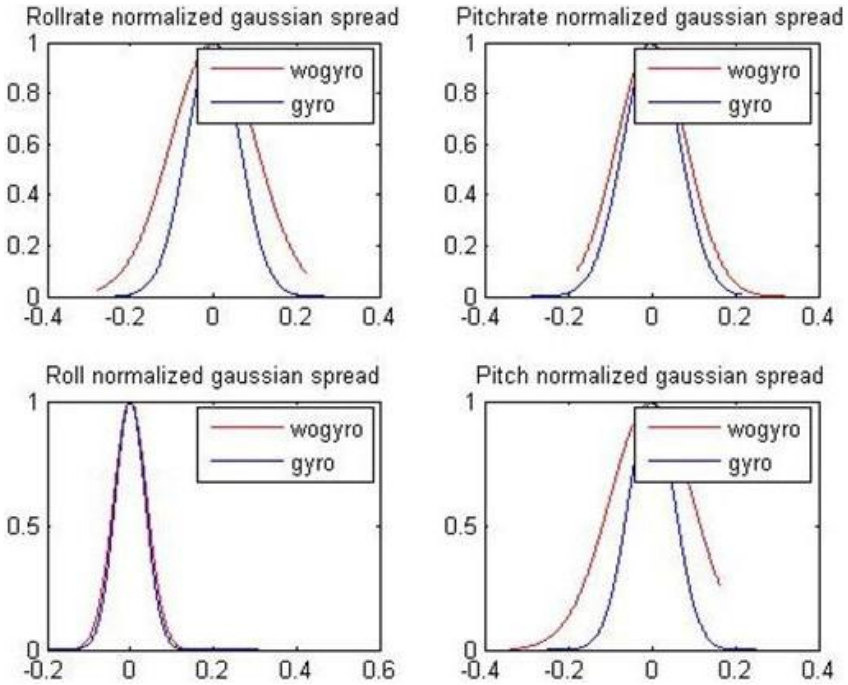

Figure 13 Comparison of RWFR response using schemes presented for robust attitude control

V. Concluding Remarks

Here, we have presented augmented attitude controller for CSIR-CMERI's Rotary-Wing Flying Robot in hover. In this case, inter-axis coupling is neglected as the controller is developed for a quasi-stable state. To compensate for errors caused by the deficiency of full knowledge of robot dynamics within the flight envelope required for hover, the results show performance of a standard attitude controller is not responsive enough to small perturbations. Therefore, cascade control loop architecture with Kalman filter-based attitude estimator featuring optimal approximation for compensating against the error caused by the deficiency of full knowledge of rotary wing robot dynamics is adopted to attain a high bandwidth for ensuring attitude stability with accelerated response for steady hover.

ACKNOWLEDGEMENT

The authors would like to thank the members of the project team on "Developing Autonomous Flying Capability of a Tele-operated Flying Robot for Inspection and Surveillance" under CSIR-CMERI SUPRA project in the 11th Five Year Plan, for their help and support. The authors would like to express their sincere gratitude to the Director of the Institute for his assent in publishing this work.

REFERENCES

[1] Jiade, W., Guoyong, H. and Yugang, F., "An attitude control method of un-manned helicopter based on adaptive output feedback, in", Proceedings of the 3rd international conference on intelligent system and knowledge engineering, Vol 1, ISKE, 2008, pp. 748–753.

[2] Sakamoto, T., Katayama, H. and Ichikawa, A., "Attitude control of a helicopter model by robust PID controllers", Proceedings of the International Symposium on Intelligent Control, IEEE, Munich, Germany, 2006. CrossRef

[3] Zhou, F., Jiande, W. and Ping, L., "Control system design and flight testing for a miniature unmanned helicopter", Proceedings of the 7th World Congress on intelligent control and automation, WCICA, 2008, pp. 2315–2319.

[4] Athans, M. and Falb, P., Optimal control - an introduction to the theory and its applications, Dover Publications, 2007.

[5] A. E. Bryson and Y.-C. Ho, Applied optimal control - optimization, estimation and control, Taylor and Francis Group, 1975.

[6] Datta, S., Patkar, U. S. and Majumder S., "Digital controller for attitude control of rotary-winged flying robot in hover," Proceeding of International Symposium on Industrial Electronics ISIE 2009, IEEE, 2009, pp. 390 –395.